

# SCIENTIFIC REPORTS



OPEN

## C-terminus of HSC70-Interacting Protein (CHIP) Inhibits Adipocyte Differentiation via Ubiquitin- and Proteasome-Mediated Degradation of PPAR $\gamma$

Received: 18 May 2016  
Accepted: 01 December 2016  
Published: 06 January 2017

Jung-Hoon Kim, Soyeon Shin, Jinho Seo, Eun-Woo Lee, Manhyung Jeong, Min-sik Lee, Hyun-Ji Han & Jaewhan Song

PPAR $\gamma$  (Peroxisome proliferator-activated receptor  $\gamma$ ) is a nuclear receptor involved in lipid homeostasis and related metabolic diseases. Acting as a transcription factor, PPAR $\gamma$  is a master regulator for adipocyte differentiation. Here, we reveal that CHIP (C-terminus of HSC70-interacting protein) suppresses adipocyte differentiation by functioning as an E3 ligase of PPAR $\gamma$ . CHIP directly binds to and induces ubiquitylation of the PPAR $\gamma$  protein, leading to proteasome-dependent degradation. Stable overexpression or knockdown of CHIP inhibited or promoted adipogenesis, respectively, in 3T3-L1 cells. On the other hand, a CHIP mutant defective in E3 ligase could neither regulate PPAR $\gamma$  protein levels nor suppress adipogenesis, indicating the importance of CHIP-mediated ubiquitylation of PPAR $\gamma$  in adipocyte differentiation. Lastly, a CHIP null embryo fibroblast exhibited augmented adipocyte differentiation with increases in PPAR $\gamma$  and its target protein levels. In conclusion, CHIP acts as an E3 ligase of PPAR $\gamma$ , suppressing PPAR $\gamma$ -mediated adipogenesis.

Diabetes mellitus is closely related to other metabolic, cardiac, inflammatory, and osteogenic diseases<sup>1–3</sup>. In particular, glucose intolerance triggered by obesity is one of the major causes of diabetes mellitus and related diseases<sup>4,5</sup>. Adipocytes play key roles in maintaining homeostasis of lipids and glucose throughout the body by storing triglycerides and secreting various cytokines and adipokines, including adiponectin and leptin<sup>6</sup>. Thus, understanding the process of adipocyte differentiation is a key step in preventing and overcoming metabolic diseases induced by obesity.

PPAR $\gamma$  is a master transcriptional regulator of adipocyte differentiation, which affects lipid and glucose metabolism<sup>7,8</sup>. While its expression is observed in other tissues, PPAR $\gamma$  is predominantly expressed in adipose tissues<sup>9</sup>. PPAR $\gamma$  is both necessary and sufficient for converting pre-adipocytes to adipocytes; this has been demonstrated in PPAR $\gamma$ -knockout mice, which fail to generate adipocytes on a high-fat diet<sup>10</sup>. Because of the clinical and pathological implications in obesity, diabetes, inflammation, and cancer, PPAR $\gamma$  agonists have been developed in an attempt to treat these diseases<sup>11</sup>. The thiozolidindione (TZD) family, including troglitazone, rosiglitazone, and pioglitazone, are the most well-known PPAR $\gamma$  agonists<sup>12,13</sup>. However, side effects of these drugs include weight gain and heart and liver failure<sup>14,15</sup>. As these side effects prevent the use of TZD-related drugs, non-agonistic compounds capable of regulating PPAR $\gamma$  activation without side effects are currently being sought. Additional research efforts seek to unravel and understand the regulatory mechanisms of PPAR $\gamma$ -related pathways.

C/EBP $\alpha$  (CCAAT/enhancer-binding protein) and PPAR $\gamma$  are co-stimulators, each functioning as a transcription factor to activate the gene expression of the other<sup>16–19</sup>. Various target genes of PPAR $\gamma$ , such as *aP2* (fatty acid-binding protein), *LPL* (lipoprotein lipase), *CD36*, and *adiponectin* are induced by PPAR $\gamma$  bound to RXR (retinoid X receptor alpha)<sup>9,20</sup>. On the other hand, PPAR $\gamma$  function is negatively regulated through direct interaction with its corepressor, NcoR1<sup>21</sup>. Recently, several papers have highlighted the importance of the post-translational

Department of Biochemistry, College of Life Science and Biotechnology, Yonsei University, Seoul, 120-749, Republic of Korea. Correspondence and requests for materials should be addressed to J.S. (email: jso678@yonsei.ac.kr)

modification (PTM) of PPAR $\gamma$  in regulating metabolic disorders<sup>20,22,23</sup>. For example, MAPK (mitogen-activated protein kinases) and CDK7/9 (Cyclin-dependent kinase7/9) mediate the phosphorylation of PPAR $\gamma$ 2 at serine 112, which leads to suppression of adipocyte differentiation<sup>24</sup>. Accordingly, mutation of serine 112 to alanine in a mouse model improves insulin sensitivity in diet-induced obesity<sup>25</sup>. Another well-known phosphorylation site is serine 273, which is activated by CDK5<sup>26</sup>. Mutation of serine 273 in mice led to significant improvements in insulin resistance<sup>26</sup>. Deacetylation and sumoylation of PPAR $\gamma$  by Sirt1 (Sirtuin 1) and Ubc9 (ubiquitin carrier protein 9), respectively, also revealed intricate PTMs that modulate PPAR $\gamma$  regulation<sup>27,28</sup>. Furthermore, several E3 ligases, including MRKN1, Siah2, and Nedd4-1, are involved in ubiquitylation of PPAR $\gamma$ <sup>29–31</sup>.

CHIP (C-terminus of HSC70-interacting protein) is an E3 ligase with a variety of target proteins, including p53, PTEN (Phosphatase and tensin homolog), Tau, and RIPK3 (Receptor-interacting serine/threonine-protein kinase 3)<sup>32–35</sup>. It contains a U-box domain responsible for ubiquitylation activities and a tetratricopeptide repeat (TPR) domain required for protein interactions. In particular, the TPR region is involved in HSP70 (heat shock proteins 70) and Hsp90 (heat shock proteins 90) association<sup>36</sup>. By interacting with molecular chaperones that affect the E3 ligase function in negative or positive ways, CHIP seems to be an essential factor for the maintenance of protein homeostasis. In this paper, we identified a new physiological role of CHIP: regulation of adipocyte differentiation. CHIP induces ubiquitylation and degradation of the PPAR $\gamma$  protein through direct interaction. To confirm this, we show that stable overexpression of CHIP in 3T3-L1 cells suppresses adipocyte differentiation, while CHIP knockdown promotes adipogenesis. In accordance with these observations, CHIP-null mouse embryonic fibroblasts exhibited increased adipocyte differentiation with elevated levels of PPAR $\gamma$ . These results confirm the role of CHIP in suppressing adipogenesis by inducing degradation of the master adipocyte transcription factor PPAR $\gamma$ .

## Results

**CHIP interacts with PPAR $\gamma$ .** In previous reports, CHIP was found to be capable of modulating the activities of several nuclear receptors, including ARs (Androgen Receptors), ERs (Estrogen Receptors), and GRs (glucocorticoid receptors)<sup>37–39</sup>. This led us to investigate the impact of CHIP on the nuclear receptor PPAR $\gamma$ . We first found that CHIP was able to interact with PPAR $\gamma$ 2, a PPAR $\gamma$  isoform, under both exogenous conditions (Fig. 1a,b–d). Endogenous CHIP and PPAR $\gamma$  were also able to bind to each other in both PC-3 and 3T3-L1 cell lines (Fig. 1c,d). Supporting these observations, recombinant GST (glutathione s-transferase)-CHIP was able to bind PPAR $\gamma$ 2 that had been transcribed and translated in reticulocyte lysates, indicating a possible direct interaction between the two proteins (Fig. 1e). PPAR $\gamma$ 1, another isoform of PPAR $\gamma$ , exhibited similar CHIP-binding capabilities, implying that CHIP may not distinguish between the two isoforms of PPAR $\gamma$  (Supplemental Fig. 1a). To identify the domain responsible for these interactions, we generated several deletion mutants of either PPAR $\gamma$ 2 or CHIP and conducted immunoprecipitation analyses. Results showed that CHIP binds to multiple regions of PPAR $\gamma$ 2, including DNA- and ligand-binding domains (Fig. 1f). The CHIP TPR region is required for the interaction with PPAR $\gamma$ 2 (Fig. 1g). Of note, an E3 ligase-defective mutant, H260Q, was able to bind to PPAR $\gamma$ 2, while K30A, a mutant defective in the TPR domain, could not, corroborating the finding that the TPR region is required for the interaction between CHIP and PPAR $\gamma$ 2 (Fig. 1h)<sup>40</sup>.

**CHIP is an E3 ligase of PPAR $\gamma$ .** To observe the effect of CHIP on PPAR $\gamma$  activity, we assessed the activity of a peroxisome proliferator response element (PPRE) promoter-driven luciferase stimulated by PPAR $\gamma$ 2 with or without CHIP expression. When PPAR $\gamma$ 2 was overexpressed, luciferase activity was doubled, an effect that was inhibited by simultaneous overexpression of CHIP. Importantly, the E3 ligase-defective mutant version of CHIP, H260Q, was not able to suppress PPAR $\gamma$ 2 transcription factor activity, implying that post-translational modification processes may be required for the CHIP and PPAR $\gamma$  interaction. The similar effects were observed under the treatment of troglitazone, a artificial ligand of PPAR $\gamma$  (Fig. 2a). The elimination of CHIP using two different CHIP siRNAs in PC3 cells resulted in increased PPAR $\gamma$  protein without altering mRNA levels, indicating that CHIP may in fact regulate PPAR $\gamma$  post-translationally (Fig. 2b).

As CHIP is an E3 ligase and its elimination led to an increase in PPAR $\gamma$  protein, we next tested whether CHIP induced the degradation of PPAR $\gamma$ . Results demonstrated that overexpression of CHIP did indeed induce endogenous and exogenous PPAR $\gamma$  degradation (Fig. 2c and Supplemental Fig. 2a). CHIP-mediated degradation of endogenous PPAR $\gamma$  appears to be proteasome dependent, as degradation is blocked by MG132, a proteasome inhibitor in both 3T3-L1 and PC3 cell lines (Fig. 2d,e). Furthermore, while H260Q, the E3 ligase-defective mutant of CHIP, was able to bind PPAR $\gamma$ 2, it was incapable of inducing degradation of endogenous PPAR $\gamma$ , indicating that ubiquitylation is also required (Figs 1h and 2d,e). We observed the similar effects with overexpressed proteins including PPAR $\gamma$ 2 and CHIP or H260Q (Supplementary Figure 2b,c). Supporting this, the half-life of PPAR $\gamma$ 2 was reduced only by wild-type (WT) CHIP, not H260Q (Fig. 2f). Results for PPAR $\gamma$ 1 were similar to those for PPAR $\gamma$ 2 (Supplemental Fig. 1b,c). Overall, our results indicate that CHIP may regulate PPAR $\gamma$  via post-translational modification.

Since CHIP is a well-known E3 ligase, we next examined whether CHIP mediates the ubiquitylation of PPAR $\gamma$ . We found that poly-ubiquitylation of PPAR $\gamma$ 2 increased because of CHIP overexpression, with or without MG132 (Fig. 3a). In accordance with these observations, endogenous poly-ubiquitylated forms of PPAR $\gamma$  were reduced by the elimination of CHIP in PC3 cell lines, indicating that CHIP regulates PPAR $\gamma$  endogenously. Here, cells were treated with troglitazone to induce accumulation of PPAR $\gamma$  so that ubiquitylated forms could be detected, as previously reported (Fig. 3b)<sup>29</sup>. As a result, poly-ubiquitylated forms of endogenous PPAR $\gamma$  were also reduced following CHIP knockdown in 3T3-L1 cells that were induced to differentiate into adipocytes by treatment with dexamethasone, IBMX, and insulin (DMI treatment) for two days (Fig. 3c). As with CHIP-mediated degradation of PPAR $\gamma$ 2, the E3 ligase activity of CHIP was required for this regulation, as H260Q was not able to induce ubiquitylation of PPAR $\gamma$ 2 (Fig. 3d). Finally, using recombinant CHIP, H260Q, and PPAR $\gamma$ 2, we confirmed

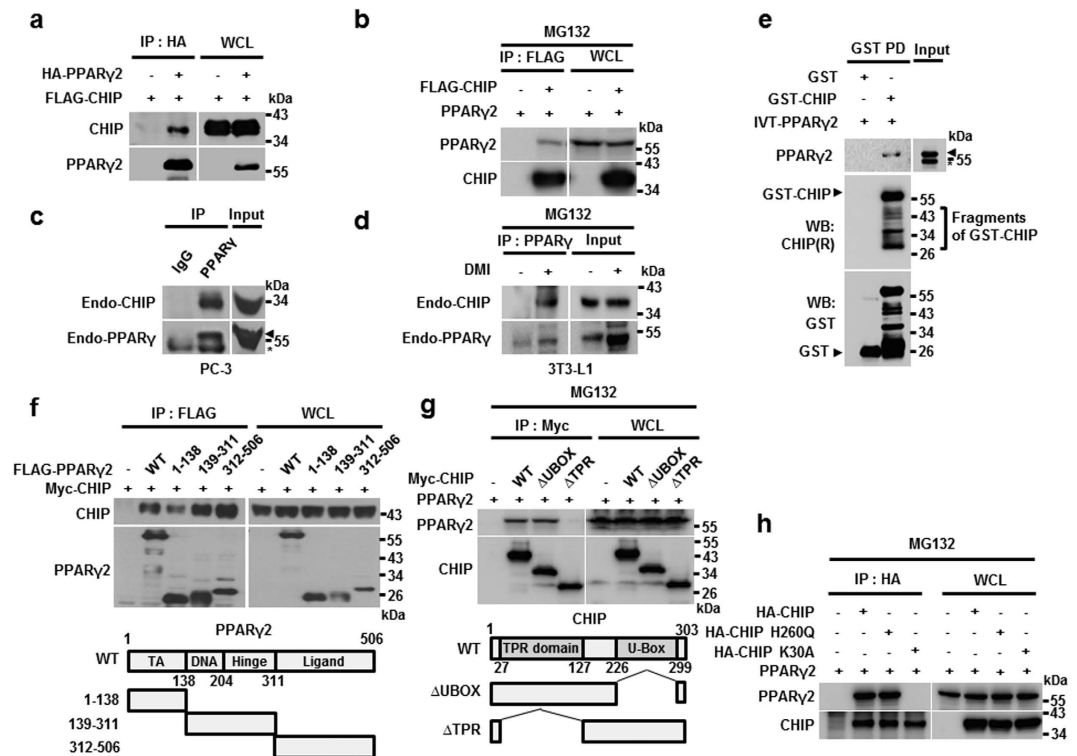


**Figure 1. CHIP interacts with PPAR $\gamma$ .** (a) CHIP binds PPAR $\gamma$  proteins to each other. Lysates of HEK293T cells transfected with pcDNA3-FLAG-CHIP and pcDNA3-HA-PPAR $\gamma$  were immunoprecipitated with  $\alpha$ -HA and FLAG antibodies. (b) PPAR $\gamma$  binds to CHIP protein reciprocally. HEK293T cells transfected with expressing vector of CHIP and PPAR $\gamma$  were treated with 10  $\mu$ M MG132 before harvest for 6 hour. (c–e) CHIP directly interacts with PPAR $\gamma$  according to endogenous and *in vitro* binding assays. (c) PC-3 cells were immunoprecipitated with  $\alpha$ -IgG and  $\alpha$ -PPAR $\gamma$ , followed by a western blot with polyclonal CHIP and monoclonal PPAR $\gamma$  antibodies. Asterisk indicates a non-specific band. (d) Preadipocyte, 3T3-L1 cells were treated with DMI cocktail (Dexamethasone, IBMX and Insulin) during 6 days. Differentiated cells were treated with MG132 for 6 h before harvest. Harvested cells were immunoprecipitated with polyclonal PPAR $\gamma$  antibody. Lysates were analyzed by western blotting indicated antibodies. (e) GST- and recombinant GST-tagged CHIP proteins were assessed with GST pull-down assay. Western blot was performed on lysates using monoclonal GST and PPAR $\gamma$  antibodies. Asterisk indicates a non-specific band. (f,g) PPAR $\gamma$  binds to the C-terminal region of the CHIP protein, and CHIP binds to the C-terminal region of the PPAR $\gamma$  protein. Lysates of HEK 293 T cells transfected with the indicated plasmids were immunoprecipitated with  $\alpha$ -Myc and  $\alpha$ -FLAG antibodies, and western blots were performed using the indicated antibodies. (h) The CHIP H260Q mutant also binds to the PPAR $\gamma$  protein. Lysates of HEK 293 T cells transfected with HA-CHIP, HA-CHIP H260Q, and FLAG-PPAR $\gamma$  expression vectors were immunoprecipitated with  $\alpha$ -HA antibodies, and western blots were performed using the indicated antibodies.

that CHIP directly ubiquitylates PPAR $\gamma$ 2 (Fig. 3e). We also observed that CHIP similarly mediates the ubiquitylation of PPAR $\gamma$ 1, supporting the conclusion that CHIP induces degradation of PPAR $\gamma$  (Supplemental Fig. 3). In summary, CHIP functions as an E3 ligase by inducing the ubiquitylation and proteasome-dependent degradation of PPAR $\gamma$ .

**HSP70 suppresses CHIP-mediated PPAR $\gamma$  degradation and ubiquitylation.** Hsp90 and Hsp70 function as major CHIP partners in the regulation of various target proteins<sup>41,42</sup>. Ubiquitylation analyses with recombinant proteins in the absence of Hsp70 and Hsp90, however, suggest that these two molecular chaperones may not participate in the CHIP-mediated ubiquitylation of PPAR $\gamma$  (Fig. 3e). To examine the roles of both molecular chaperones in PPAR $\gamma$  degradation processes further, the effect of geldanamycin (GA), an Hsp90 inhibitor, on CHIP-mediated degradation of PPAR $\gamma$  was assessed. Treatment with this inhibitor had little effect on the CHIP-mediated degradation of PPAR $\gamma$ , indicating that HSP90 may not be required for the degradation process (Supplemental Fig. 4). In contrast, transient overexpression of HSP70 inhibited CHIP-mediated degradation of PPAR $\gamma$  (Fig. 4a). While it seems that HSP70 has little effect on the binding affinity between CHIP and PPAR $\gamma$ 2, the presence of HSP70 prevents CHIP-mediated PPAR $\gamma$ 2 ubiquitylation (Fig. 4b,c). These results indicate that of the two major partners of CHIP, only Hsp70 functions as a negative regulator by suppressing CHIP-mediated ubiquitylation of PPAR $\gamma$ 2.

**CHIP suppresses adipocyte differentiation induced by PPAR $\gamma$  activation.** Because CHIP destabilizes the PPAR $\gamma$  protein via ubiquitylation and proteasome-dependent degradation, we next tested whether

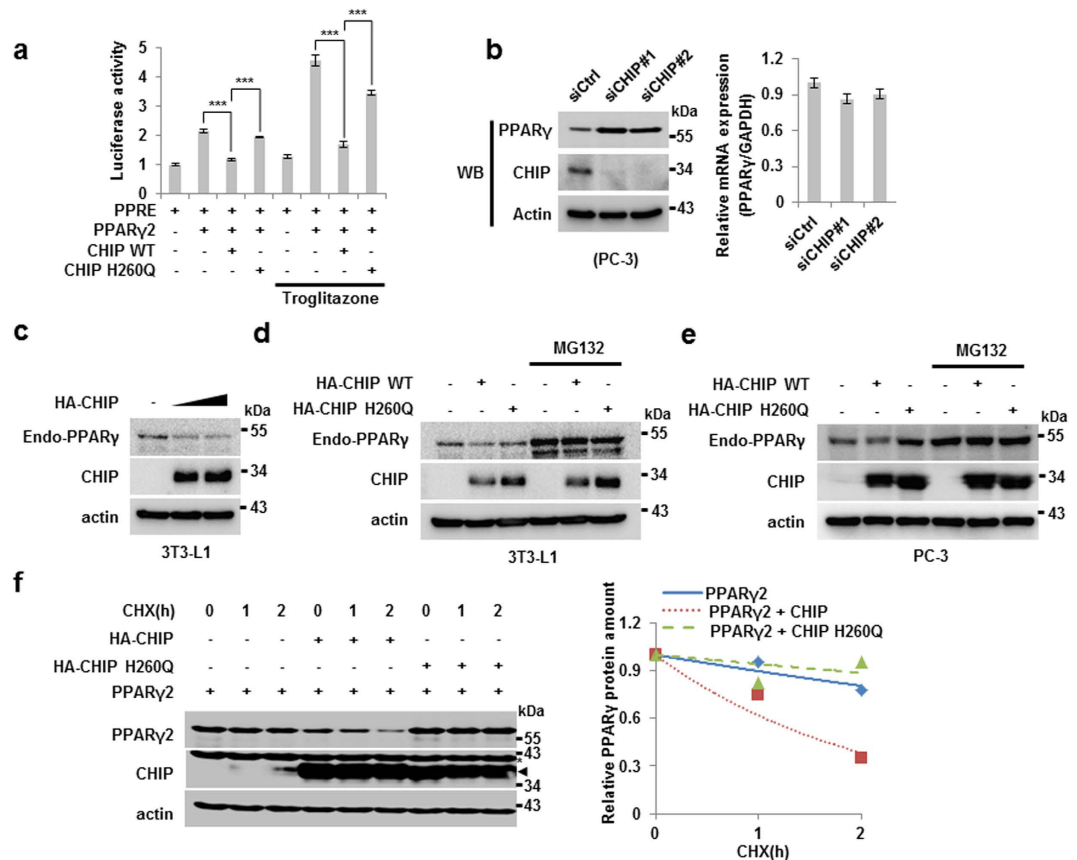


**Figure 2. CHIP degrades PPAR $\gamma$  protein through the proteasomal pathway via an E3-ligase function.** (a) CHIP represses the transcriptional activity of PPAR $\gamma$ . H1299 cells were transfected with PPRE, pcDNA3.1-PPAR $\gamma$ 2, pcDNA3-FLAG-CHIP, and pcDNA3-FLAG-CHIP H260Q plasmids with or without troglitazone. Cells were measured by luminometer. Data are presented means  $\pm$  SD;  $n = 3$ ;  $**P < 0.01$ , and  $***P < 0.001$  compared to each lane. (b) The CHIP protein level was increased by CHIP knockdown using siRNAs. Western blots of lysates of PC-3 cells transfected with the indicated plasmids using siRNA IMAX were performed using the indicated antibodies. (c) Endogenous PPAR $\gamma$  protein was degraded by CHIP. Preadipocyte, 3T3-L1 cells were treated with DMI cocktail for 2 days, were transfected with pcDNA3-HA-CHIP plasmid dose dependent manner. Indicated protein was measured by western blotting. (d,e) CHIP degrades PPAR $\gamma$  protein through the E3-ligase function and proteasomal manner. (d) DMI treated 3T3-L1 cells were transfected with HA-CHIP and HA-CHIP H260Q mutant expressing vectors with or without MG132. Each protein was detected by western blotting indicated antibodies. (e) PC-3 cells were transfected with pcDNA3-HA-CHIP and pcDNA3-HA-CHIP H260Q mutant with or without MG132. Lyzed cells were analyzed by western blotting indicated antibodies. (f) The PPAR $\gamma$  protein was destabilized by wild-type CHIP but not by the H260Q mutant. Western blots of H1299 cells transfected with plasmids expressing PPAR $\gamma$ , FLAG-CHIP, and FLAG-CHIP H260Q in the presence or absence of 50  $\mu$ g/mL CHX (cycloheximide) treatment were performed using the indicated antibodies and were measured with the Image J program. Asterisk indicates an actin band.

CHIP is able to regulate adipocyte differentiation in 3T3-L1 cells. First, we generated 3T3-L1 cell lines that stably overexpress CHIP or H260Q using a retroviral system. Along with a control cell line transfected with pBABE, these cell lines were induced to differentiate into adipocytes through DMI treatment. Oil Red O staining data and quantification of lipid content showed that the cell line overexpressing CHIP displayed reduced levels of adipogenesis compared to both the control and H260Q-transfected cells (Fig. 5a,b). We next examined the protein and mRNA levels of PPAR $\gamma$  and its targets in the same cell lysates. As expected, cells overexpressing CHIP exhibited reductions in both PPAR $\gamma$  mRNA and protein levels. We also observed reductions in the PPAR $\gamma$  targets aP2, cofactor C/EBP $\alpha$  and CD36 in cells overexpressing CHIP (Fig. 5c–d). We further generated 3T3-L1 cell lines with stable knockdown of CHIP (shCHIP#3, shCHIP#4) using a lentiviral vector system. In contrast to the overexpression system, stable cell lines with CHIP knockdown displayed more adipocyte differentiation than that of control cells (shGFP) detected by Oil Red O staining (Fig. 6a), and this was confirmed by quantification of lipid content (Fig. 6b). The cell lines expressing shCHIP#3 and shCHIP #4 were further analyzed by western blot and qRT-PCR. Like PPAR $\gamma$ , aP2, C/EBP $\alpha$  and CD36 were elevated following CHIP knockdown when compared to control cells (Fig. 6c,d). Finally, WT or CHIP-null MEFs were employed to examine the effects of CHIP on adipocyte differentiation induced by DMI plus troglitazone, a PPAR $\gamma$  ligand<sup>29</sup>. Two CHIP knockout MEFs, CHIP KO #6 and CHIP KO #9, exhibited greater adipocyte differentiation than the two wild-type MEFs, WT #3 and

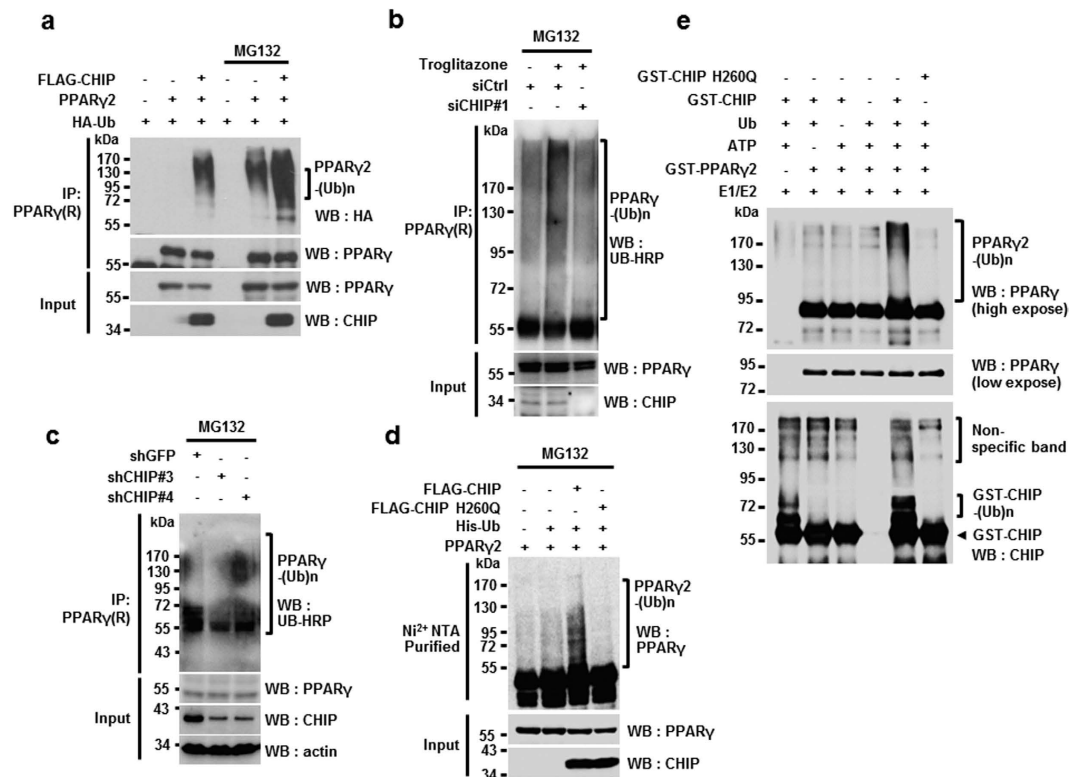


**Figure 3. CHIP mediates ubiquitylation of PPAR $\gamma$ 2 through its E3 ligase activity.** (a) CHIP induces ubiquitylation of PPAR $\gamma$ 2. Western blots of H1299 cells transfected with pcDNA3.1-PPAR $\gamma$ , pcDNA3.1-FLAG-CHIP, and PMH-HA-Ub with or without MG132 were performed using the indicated antibodies. (b,c) Elimination of CHIP did not increase the ubiquitylation of PPAR $\gamma$ . Lysates of PC-3 cells transfected with siRNA control (siCtrl) or siRNA CHIP #1 and treated with MG132 were immunoprecipitated with polyclonal PPAR $\gamma$  antibodies and western blots were performed using the indicated antibodies. (b) Lysates of 3T3-L1 cells transfected with CHIP knockdown plasmids expressing shCHIP #3 and shCHIP #4 or control plasmid (shGFP), differentiated by DMI treatment, and treated with MG132 were immunoprecipitated using polyclonal PPAR $\gamma$ . (c) Western blots were performed on the above lysates using the indicated antibodies. (d) PPAR $\gamma$ 2 protein was ubiquitylated by wild-type CHIP but not the H260Q mutant. Western blots of H1299 cells transfected with as describe above all, with His-ubiquitin-conjugated proteins pulled down using Ni<sup>2+</sup>-NTA beads. The indicated antibodies were used. (e) CHIP directly ubiquitinates PPAR $\gamma$ 2 *in vitro*. Western blots of purified GST-PPAR $\gamma$  2 recombinant protein incubated with ATP, E1, E2, and ubiquitin in the presence or absence of wild-type GST-CHIP or GST-CHIP H260Q mutant were performed using the indicated antibodies.

#8 (Fig. 7a). The data showing quantification of lipid contents confirmed these results (Fig. 7b). Similarly, mRNA or protein levels of PPAR $\gamma$ , aP2, C/EBP $\alpha$  and CD36 were all elevated in CHIP KO #6 and CHIP KO #9 MEFs compared with those of controls (Fig. 7c,d). In summary, these data suggest that CHIP functions as a negative modulator of adipocyte differentiation in 3T3-L1 and primary MEF cells, possibly by suppressing PPAR $\gamma$ .

## Discussion

In this study, we identified a new role of CHIP in adipocyte differentiation. CHIP interacts with and mediates the ubiquitylation of PPAR $\gamma$ , which results in negative effects on adipogenesis. CHIP is commonly known to exert its E3 ligase effects in association with the molecular chaperones Hsp90 and Hsp70<sup>43</sup>. For example, Hsp70 facilitates the CHIP-mediated degradation of p53, HIF-1 $\alpha$ , and AR<sup>32,37,41</sup>, while Hsp90 is known to suppress CHIP-mediated degradation by promoting the stability of CHIP target proteins<sup>44,45</sup>. Notably, PPAR $\gamma$  degradation induced by CHIP does not seem to require the presence of either Hsp90 or Hsp70. The poly-ubiquitylation of PPAR $\gamma$  occurs independently of the molecular chaperones, as demonstrated by ubiquitylation analyses with recombinant proteins. The inhibition of Hsp90 by geldanamycin does not have a strong effect on CHIP-mediated PPAR $\gamma$  degradation. Interestingly, it has been reported that Hsp90 inhibition leads to suppression of adipogenesis<sup>46</sup>. Based on our results, it appears that Hsp90 may regulate adipocyte differentiation via a CHIP-independent regulatory pathway. In contrast, Hsp70 appears to function as a negative regulator of CHIP-dependent PPAR $\gamma$  degradation. Upon expression of Hsp70, both the ubiquitylation and degradation of PPAR $\gamma$  were suppressed. A similar pathway, in which Hsp70 functions as a negative regulator of CHIP, can be found in the CHIP-dependent degradation of Tau<sup>34</sup>. In this case, CHIP-mediated ubiquitylation of Tau is suppressed by Hsp70. Since Hsp70 suppresses the function of CHIP, it may function as a positive regulator in adipogenesis by stabilizing PPAR $\gamma$ . Further physiological studies on the role of Hsp70 in adipocyte differentiation and its systemic effects should be conducted in the future.

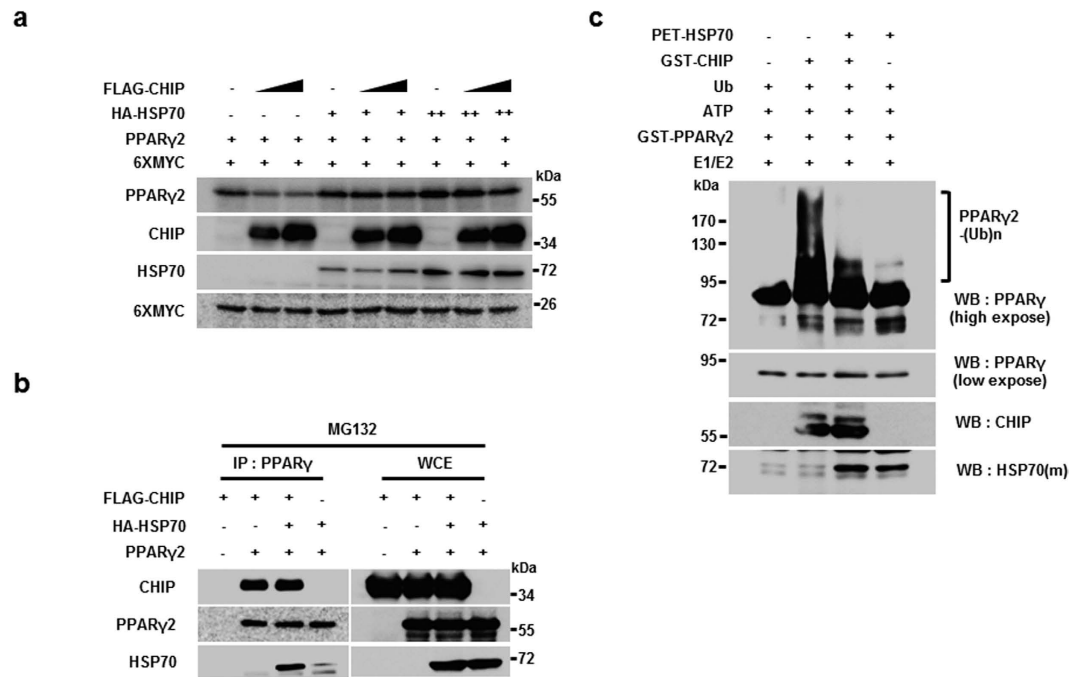


**Figure 4. HSP70 suppresses CHIP E3 ligase activity, reducing PPAR $\gamma$ 2 degradation.** (a) CHIP-mediated PPAR $\gamma$ 2 degradation was blocked by HSP70. Western blots of H1299 cells transfected with FLAG-CHIP, PPAR $\gamma$ 2, 6XMYC, and increasing amounts of HSP70-expressing plasmid were performed using the indicated antibodies. (b) Interaction between CHIP and PPAR $\gamma$ 2 was not affected by HSP70. HEK 293 T cells were transfected with pcDNA3-FLAG-CHIP, pcDNA3.1-PPAR $\gamma$ 2, and pcDNA3-HA-HSP70 in the presence of MG132 for 6 hour. Lysates of HEK 293 T cells transfected with PPAR $\gamma$ 2 and CHIP-expressing plasmids were immunoprecipitated with  $\alpha$ -PPAR $\gamma$  antibodies, and western blots were performed using the indicated antibodies. (c) HSP70 negatively regulates the E3 ligase function of CHIP, reducing PPAR $\gamma$ 2 ubiquitylation. Western blots of purified recombinant proteins (GST-PPAR $\gamma$ 2, GST-CHIP, GST-CHIP H260Q, and PET-HSP70) incubated with ATP, E1, E2, and ubiquitin were performed using the indicated antibodies.

Several other E3 ligases have been previously reported to ubiquitylate PPAR $\gamma$ . MKRN1 was the first E3 ligase known to mediate PPAR $\gamma$  ubiquitylation and degradation<sup>29</sup>. SIAH2 and NEDD4-1 were subsequently identified as E3 ligases of PPAR $\gamma$ <sup>30,31</sup>. With the addition of CHIP based on our results, it appears that PPAR $\gamma$  may be regulated by several E3 ligases. However, most of these observations occurred while investigating cellular differentiation. To determine the role of CHIP in other physiological settings, we generated CHIP-null MEFs and compared differentiation in WT and CHIP-null MEFs. The results demonstrated that CHIP-null MEFs differentiated into adipocytes more effectively than WT MEFs, supporting our *in vitro* data (Figs 1–3). Based on these observations, the systemic effects of CHIP should be further assessed in the future. Since the whole-body CHIP knockout mouse of the C57BL/6 strain does not survive for more than one month, a conditional knockout system must be established to investigate the physiological roles of CHIP in association with PPAR $\gamma$ <sup>35,47</sup>. Additional studies should examine whether the E3 ligases identified so far are expressed in adipocyte tissues and whether their expression levels are regulated by a high-fat diet. Any E3 ligase whose expression is negatively correlated with that of PPAR $\gamma$  under high-fat diet conditions may be a good candidate for drug targeting<sup>48</sup>. Further *in vivo* studies utilizing high-fat-diet induced mice may indicate the main E3 ligase of PPAR $\gamma$ .

TZD and its analogs have been clinically tested for treating obesity and diabetes mellitus through the agonistic activation of PPAR $\gamma$ <sup>49,50</sup>. Unfortunately, these drugs exhibited various side effects, including heart and liver failure, weight gain, fluid retention, and bone fractures<sup>51,52</sup>. As these drugs have been withdrawn from the market or removed from general usage due to their severe side effects, the concept of developing novel, non-agonistic drugs has been pursued<sup>53</sup>. As various post-translational modifications could regulate the function of PPAR $\gamma$  in possibly non-agonistic ways, targeting post-translational regulators may be a good strategy for discovering non-agonistic drugs with reduced side effects<sup>54</sup>. Since the suppression of CHIP may stabilize and activate PPAR $\gamma$ , CHIP suppression may represent a good target for clinical trials for the treatment of diabetes and obesity.

## Methods

**Adipocyte differentiation.** Pre-adipocyte 3T3-L1 cells were used to measure adipocyte differentiation. When cells were almost confluent, differentiation was induced with DMEM (dulbecco's modified eagle's medium, Corning Cellgro) containing 10% FBS (fetal bovine serum), 1% penicillin/streptomycin, IBMX (3-isobutyl-1-methylxanthine) (520  $\mu$ M), insulin (1  $\mu$ g/mL), and dexamethasone (1  $\mu$ M) (DMI treatment) for two days. The medium was changed to DMEM containing insulin for an additional two days. On day 4, further differentiation was induced by changing the medium to FBS only. MEF cells were generated as previously described<sup>29</sup>. In

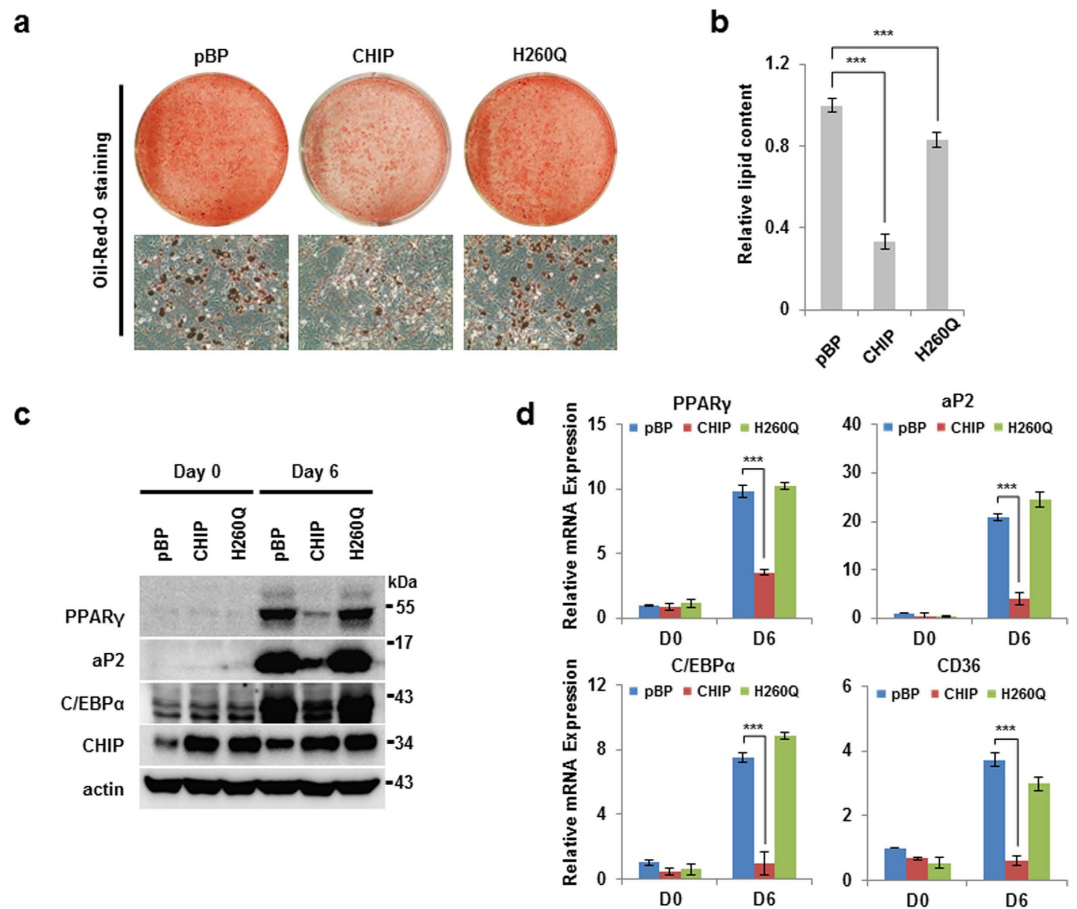


**Figure 5. CHIP inhibits adipocyte differentiation in 3T3-L1 cells.** (a,b) CHIP-overexpressing cells were suppressed during adipogenesis compared to control cells. Preadipocyte 3T3-L1 cells were generated by pBAGE puro, pBP-CHIP, and pBP-CHIP H260Q-expressing viral vectors using a virus infection system and were differentiated using a DMI cocktail (dexamethasone, IBMX, insulin). (a) Differentiated cells were stained by Oil Red O and were photographed under the microscope. (b) Differentiated cells were measured by quantification of lipid content assay using the assay kit. (c,d) Protein expression and mRNA of PPAR $\gamma$  included its targets were reduced in CHIP-overexpressing cells. Western blots of lysed differentiated cells were performed using the indicated antibodies and measured by PPAR $\gamma$  or its target mRNA using qRT-PCR. Data are presented means  $\pm$  SD; n = 3; \*\*\*P < 0.001 compared with pBP.

the case of adipocyte differentiation of MEF cells, troglitazone was added as a PPAR $\gamma$  ligand during each step. Fully differentiated adipocyte cells were detected under a microscope by Oil Red O staining. Stained cells were extracted with isopropanol. Extracted stains were measured by microplate reader for quantification of differentiation density.

**Cell culture.** H1299, 293FT, and MEF cells were maintained in DMEM containing 10% FBS (Corning Cellgro) and 1% penicillin/streptomycin (Gibco, NY, USA). PC-3 cells were cultured in RPMI (Hyclone) supplemented with 10% FBS (Corning Cellgro). NIH 3T3-L1 cells were maintained in DMEM (Gibco) with 10% calf bovine serum (Gibco) and 1% penicillin/streptomycin (Gibco). We purchased the 293FT cell line from Invitrogen, and the 3T3-L1 and H1299 cell lines were purchased from ATCC (American Type Culture Collection). PC-3 cells were provided by Kyung-sup Kim (Yonsei University College of Medicine, Seoul).

**Generation of mouse fibroblast cells.** All of mouse experiments were approved by The Institutional Animal Care and Use Committees of Yonsei University (IACUC-A-201409-294-01). The mice were maintained in accordance with the approved guidelines and regulations for experimental animals provided by Yonsei Laboratory Animal Research Center. Using C57BL/6 J mice, heterogeneous CHIP male and female mice were mated to produce wild type and knockout CHIP mice, as previously reported<sup>35</sup>. Mouse embryos were obtained 13.5 days after verifying plug formation. Embryos were minced with a blade in 1 ml trypsin-EDTA. Cells were transferred to 150-mm plates containing DMEM medium with 10% FBS. After 16 hours, cells were maintained in DMEM medium.

**Plasmids.** The following constructs were used: pcDNA3.1-PPAR $\gamma$ 1, pcDNA3.1-PPAR $\gamma$ 2, pCS4-3xHA-PPAR $\gamma$ 2, pCS4-3xFLAG-PPAR $\gamma$ 2, pGEX-4T1-PPAR $\gamma$ 2, pTK-PPREx3-luc, pBabe-puro, pcDNA3-His-Ub, and

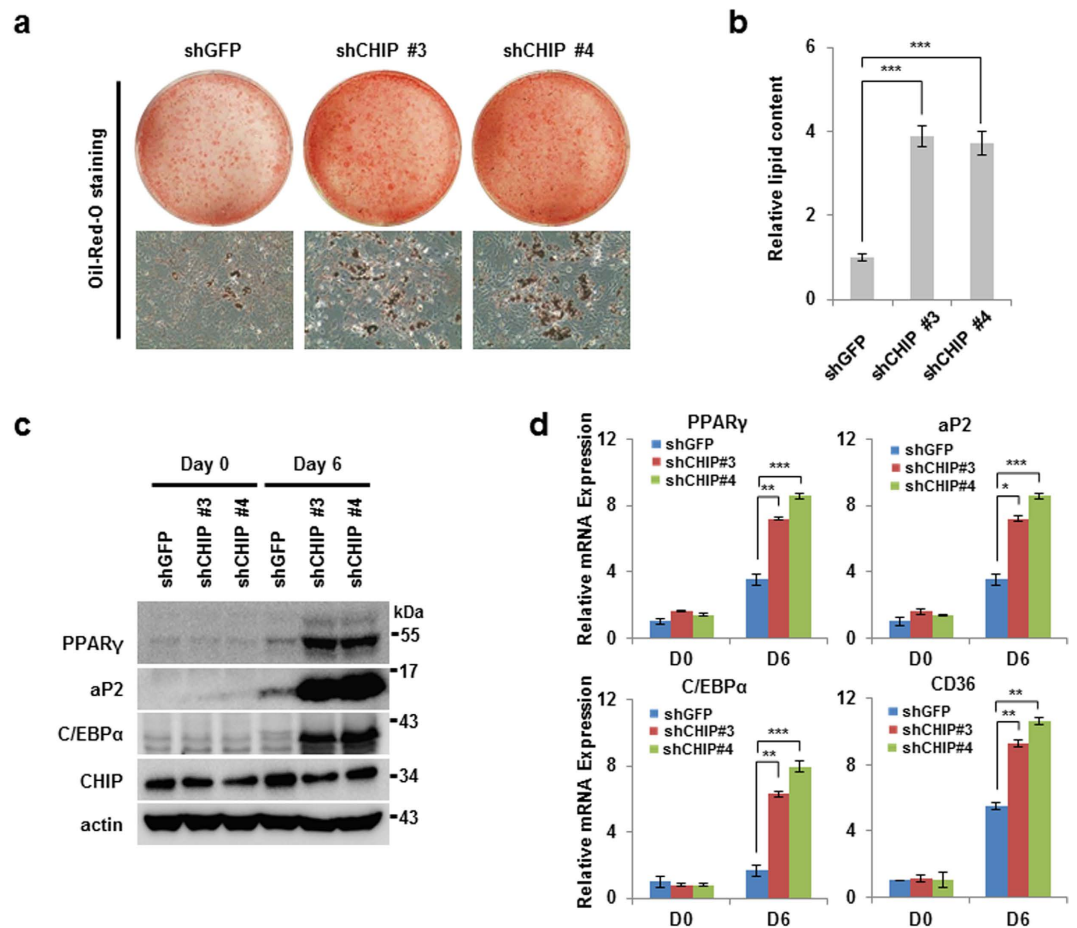


**Figure 6. Knockdown of CHIP induces adipocyte differentiation in 3T3-L1 stable cells.** (a,b) Elimination of CHIP accelerates adipocyte differentiation in 3T3-L1 cells. 3T3-L1 cells were infected by CHIP-knockdown lentivirus shRNA (shGFP, shCHIP #3, shCHIP #4) and were differentiated by DI (Dexamethasone and Insulin) cocktail. Differentiated cells were stained and measured as in Fig. 5. (c,d) PPAR $\gamma$  mRNA and protein levels increased in CHIP-knockdown 3T3-L1 cells. Western blots and qRT-PCR of differentiated cells were performed using the indicated antibodies and primers. Data are presented means  $\pm$  SD; n = 3; \*P < 0.05, \*\*P < 0.01, and \*\*\*P < 0.001 compared with shGFP.

pHM6-HA-Ub<sup>29</sup>. In addition, we used the following CHIP plasmids, which have been previously described<sup>35</sup>: pcDNA3-FLAG-CHIP, pcDNA3-FLAG-CHIP H260Q, pcDNA3-MYC-CHIP, pcDNA3-MYC-CHIP  $\Delta$ UBOX, pcDNA3-MYC-CHIP  $\Delta$ TPR, pGEX-4T1-CHIP, and pGEX-4T1-CHIP H260Q. Other CHIP constructs (pcDNA3-HA-CHIP, pcDNA3-HA-CHIP H260Q, and pcDNA3-HA-CHIP K30A) were sub-cloned from pcDNA3-FLAG-CHIP. An HA-HSP70 expressing plasmid (pcDNA3-HA-HSP70) was generated by polymerase chain reaction followed by insertion into pcDNA3-HA. The PET-HSP70 plasmid has been described previously<sup>55</sup>.

**Antibodies and chemicals.** The following antibodies were used in this study for western blots and immunoprecipitation assays: anti-CHIP (rabbit C3B6; Cell Signaling Technology, Danvers, Massachusetts, USA), MYC (sc-40; Santa Cruz Biotechnology, CA, USA), FLAG (mouse F3165; Sigma-Aldrich, St. Louis, MO, USA), FLAG (rabbit; Sigma-Aldrich), HA (mouse sc-7392; Santa Cruz Biotechnology, CA, USA), PPAR $\gamma$  (mouse sc-7273X, Santa Cruz Biotechnology), PPAR $\gamma$  (rabbit sc-7196X; Santa Cruz Biotechnology), aP2 (goat sc-18661; Santa Cruz Biotechnology), C/EBP $\alpha$  (rabbit sc-61X; Santa Cruz Biotechnology),  $\beta$ -actin (A5316; Sigma-Aldrich), MG132 (M-1157, A.G. Scientific, San Diego, CA, USA), and geldanamycin (9843 S, Cell Signaling Technology). Pepstatin A (P5318), aprotinin (A1153), phenylmethanesulfonyl fluoride (PMSF; P7626), leupeptin (L2884), dimethyl sulfoxide (DMSO; D8418), N-ethylmaleimide (NEM; E3876), dexamethasone (D1756), 3-isobutyl-1-methylxanthine (IBMX; I5879), and Oil Red O (O0625) were purchased from Sigma-Aldrich (St. Louis, MO, USA), while insulin (11 376 497 001) was purchased from Roche (Mannheim, Germany).

**Transfection.** Lipofectamine 2000 (Invitrogen, Carlsbad, CA, USA) was used to transfect 293FT and H1299 cells according to the manufacturer's instructions. PC-3 cells were transfected with the siRNAs CHIP #1 (5'-CCA GCT GGA GAT GGA GAG TTA-3') and CHIP #2 (5'-CTG CGC GGG CTG CGC GCT CTA-3') using



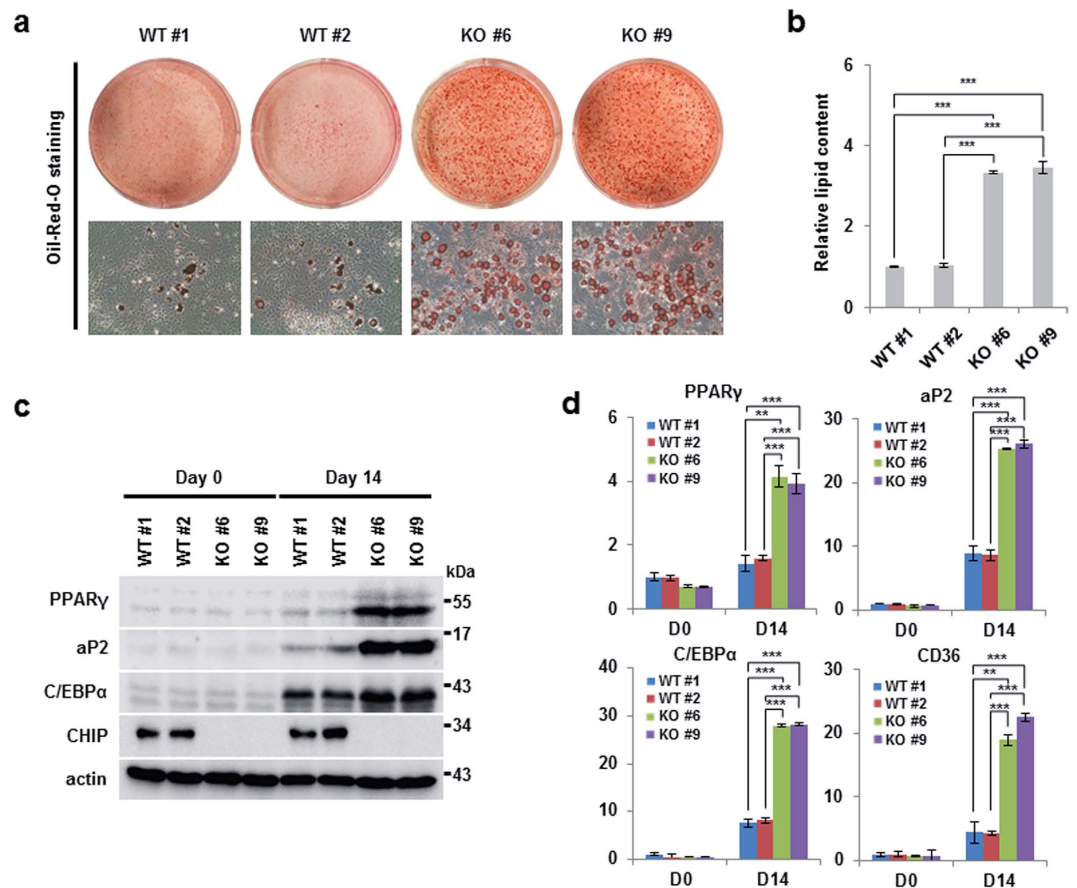


**Figure 7. Elimination of CHIP suppresses adipogenesis in mouse embryo fibroblast (MEF) cells.**

(a,b) CHIP-knockout MEFs were induced to undergo accelerated adipocyte differentiation. CHIP-knockout MEFs generated through the instrumental method were induced to undergo differentiation into adipocytes through treatment with DMI and the PPAR $\gamma$  ligand troglitazone. (a) Differentiated cells were stained using Oil Red O and were photographed as described in Fig. 5. (b) Lipid content was analyzed by quantification kit in differentiated cells. (c,d) PPAR $\gamma$  protein and mRNA levels were elevated in CHIP-knockout MEFs. (c) Western blots of differentiated MEFs were performed using the indicated antibodies. (d) Messenger RNA of PPAR $\gamma$  and its targets was detected by qRT-PCR using the indicated primers. Data are presented means  $\pm$  SD; n = 3; \*\*P < 0.01, and \*\*\*P < 0.001 compared to each lane.

Lipofectamine RNAi MAX (Invitrogen). Preadipocyte, 3T3-L1 cells were transfected with the plasmids using Viafect (Promega, Woods Hollow Road Madison, WI, USA, E4981).

**Quantitative RT-PCR analysis.** Extraction of RNA was performed using Trizol (Invitrogen) according to the manufacturer's instructions. Total cDNA was synthesized from isolated RNA using M-MLV reverse transcriptase (Takara Bio Company, Otsu, Japan). Samples were examined by quantitative PCR using a QuantiTect SYBR Green PCR Kit (Qiagen, CA, USA) and the following primers: glyceraldehyde 3-phosphate dehydrogenase (GAPDH; 5'-GGC TGC TTT TAA CTC TGG TA-3' and 5'-ACT TGA TTT TGG AGG GAT CT-3'), mouse PPAR $\gamma$  (5'-CCA TTC TGG CCC ACC AAC-3' and 5'-AAT GCG AGT GGT CTT CCA TCA-3'), human PPAR $\gamma$  (5'-TTC AGA AAT GCC TTG CAG TG-3' and 5'-CCA ACA GCT TCT CCT TCT CG-3'), aP2 (5'-CAC CGC AGA CGA CAG GAA G-3' and 5'-GCA CCT GCA CCA GGG C-3'), 36B4 (5'-AGA TGC AGC AGA TCC GCA T-3' and 5'-GTT CTT GCC CAT CAG CAC C-3'), and C/EBP- $\alpha$  (5'-GCG GGC AAA GCC AAG AA-3' and 5'-GCG TTC CCG CCG TAC C-3'). The expression level of each gene was determined from 3T3-L1 and MEF cell samples and was normalized to the expression of the 36B4 gene in the same sample. The expression levels of genes in PC-3 cells were normalized to those of GAPDH.

**Ubiquitylation assays.** H1299 cells were transfected with HA-tagged ubiquitin (PRK5-HA-ub), pcDNA3.1, and pcDNA3.1-PPAR $\gamma$  plasmids with or without pcDNA3-FLAG-CHIP and pcDNA3-FLAG-CHIP H260Q in the presence of MG132. Using PBS containing NEM (10 nM), harvested cells were lysed by boiling in 1% SDS for 10 min. Lysates were produced by adding protease inhibitors (2  $\mu$ M leupeptin, 1  $\mu$ M pepstatin A, 2  $\mu$ M aprotinin, 200  $\mu$ M PMSF) and lysis buffer with NEM to approach 0.1% SDS concentration. Samples were immunoprecipitated with monoclonal  $\alpha$ -PPAR $\gamma$  antibody and were analyzed by western blot using the indicated antibodies. To assess ubiquitylation using Ni<sup>2+</sup>-NTA beads, H1299 cells were transfected with His-tagged ubiquitin (pcDNA3-His-Ub), pcDNA3.1-PPAR $\gamma$ , pcDNA3-FLAG-CHIP, and pcDNA3-FLAG-CHIP H260Q in the presence

of MG132. Cells were harvested with NEM containing PBS and were lysed by 6 M guanidine-sodium phosphate buffer (pH 7). Samples were combined with Ni<sup>2+</sup>-NTA beads for 4 hours and were eluted by 200 mM imidazole. Western blotting was performed as described above. Endogenous ubiquitylation was analyzed in PC-3 and 3T3-L1 cells. PC-3 cells were transfected with siRNA CHIP #1 for 24 hours and were then treated with troglitazone for an additional 12 hours to induce endogenous PPAR $\gamma$  ubiquitylation. In 3T3-L1 cells, CHIP was stably knocked down with shCHIP#3 and shCHIP#4, and differentiation was induced with DMI for two days before cells were treated with MG132 for six hours. Harvested and lysed cells were immunoprecipitated with polyclonal  $\alpha$ -PPAR $\gamma$  antibody and were measured by western blot using the indicated antibodies. For *in vitro* ubiquitylation, recombinant proteins (GST-PPAR $\gamma$ 2, GST-CHIP, and GST-CHIP H260Q) were incubated with 10  $\mu$ g ubiquitin (Sigma, U6235), 2 mM ATP (Fermentas, R0441), 200 ng E1 (UBE1, Boston Biochem, E-305), and 500 ng E2 (UbcH5c, Boston Biochem, E2-627) in reaction buffer (40 mM Tris-HCl pH 7.6, 50 mM NaCl, and 1 mM DTT) for four hours at 37 °C. Samples were boiled and diluted with buffer to 0.1% SDS and then were immunoprecipitated using monoclonal  $\alpha$ -PPAR $\gamma$  antibody. Ubiquitylation of PPAR $\gamma$  was detected by western blot, as described above.

**Protein purification, *in vitro* translation, and *in vitro* binding assays.** pGEX-4T-1-CHIP, pGEX-4T-1-CHIP H260Q, and pGEX-4T-1-PPAR $\gamma$ 2 were expressed in *Escherichia coli* and purified using glutathione sepharose 4B (GE Healthcare, UK). Bacteria expressing GST-tagged proteins (GST-PPAR $\gamma$ 2, GST-CHIP, and GST-CHIP H260Q) were lysed using lysis buffer (300 mM NaCl, 25 mM sodium phosphate buffer at pH 7, 20 mM beta-mercaptoethanol, protease inhibitors, and 5% glycerol). GST-PPAR $\gamma$ 2, GST-CHIP, and GST-CHIP H260Q were purified using GST beads (GE Healthcare, UK) following the manufacturer's protocol. A His-HSP70-expressing vector (PET-HSP70) was examined via transformation into BL21 cells. Cells were lysed using Tris-HCl buffer (50 mM NaCl, 40 mM Tris-HCl at pH 7, 20 mM beta-mercaptoethanol, protease inhibitors, and 5% glycerol). Lysed protein was purified using Ni<sup>2+</sup>-NTA beads and was eluted using 250 mM imidazole. A TNT T7-coupled reticulocyte lysate system (L4610, Promega, USA) was used to produce PPAR $\gamma$ 2 protein. Translated protein was incubated with GST or GST-PPAR $\gamma$ 2 for two hours and then with sepharose beads for one hour. Complexes were then washed and eluted with reduced glutathione (10 mM), followed by western blot analysis.

**Generation of CHIP stable cell lines.** CHIP overexpression cell lines were generated using pBABE-puro-CHIP and pBABE-puro-CHIP H260Q plasmids and the packaging cell line HEK-293FT, as previously described<sup>35</sup>. All shRNA constructs were purchased from Sigma-Aldrich (St. Louis, MO, USA) with the following sequences: mouse CHIP#3 (5'-CACGATAAATACATGGCAGAT-3') and CHIP#4 (5'-GAGAGTGAGCTGCATTCATAT-3'). NIH-3T3-L1 cells stably expressing shGFP or mouse CHIP shRNA (shCHIP#3 and shCHIP#4) were established for generation of CHIP knockdown cell lines using the manufacturer's instructions. We transfected 293FT cells with lentiviral packaging vectors and pLKO.1-shGFP or shCHIP#3/#4. At 48 h post-transfection, viral supernatants were harvested, filtered, and added to 3T3-L1 cells. Infected 3T3-L1 cells were selected by puromycin treatment for seven days.

**Quantification of lipid content.** The lipid contents were measured with triglyceride quantification colorimetric/fluorometric kits (Biovision, Milpitas, CA, K622-100). Analysis of lipid contents was performed by Biovision as described. Differentiated cells were collected in PBS. Cells were homogenized with 5% NP-40 diluted with water. Lysates and triglycerides were slowly boiled at 80 to 100 °C in a water bath and then cooled down to room temperature. Triglyceride standards were used to make a standard curve. Lysed samples were incubated with lipase in the assay buffer for 20 min, and a mixture of the triglyceride probe was added to the buffer, followed by incubation for 30 to 60 min. The absorbance of the samples was measured with a microtiter plate reader at 570 nm. The values were entered into the provided formula to obtain the final results.

**Statistical analyses.** Statistical analyses were conducted using Prism (GraphPad Software Inc., CA, USA), and results are presented as means  $\pm$  SD. All statistical results in Prism were performed using unpaired two-tailed t-test to compare two groups ( $n \geq 3$ ).

## References

1. Grundy, S. M. *et al.* Diabetes and cardiovascular disease—A statement for healthcare professionals from the American Heart Association. *Circulation* **100**, 1134–1146 (1999).
2. Donath, M. Y. & Shoelson, S. E. Type 2 diabetes as an inflammatory disease. *Nat Rev Immunol* **11**, 98–107, doi: 10.1038/nri2925 (2011).
3. Rosen, C. J. & Bouxsein, M. L. Mechanisms of disease: is osteoporosis the obesity of bone? *Nat Clin Pract Rheum* **2**, 35–43, doi: 10.1038/ncprheum0070 (2006).
4. Kahn, S. E., Hull, R. L. & Utzschneider, K. M. Mechanisms linking obesity to insulin resistance and type 2 diabetes. *Nature* **444**, 840–846, doi: 10.1038/nature05482 (2006).
5. Barr, E. L. M. *et al.* Risk of cardiovascular and all-cause mortality in individuals with diabetes mellitus, impaired fasting glucose, and impaired glucose tolerance - The Australian diabetes, obesity, and lifestyle study (AusDiab). *Circulation* **116**, 151–157, doi: 10.1161/Circulationaha.106.685628 (2007).
6. Ouchi, N., Parker, J. L., Lugus, J. J. & Walsh, K. Adipokines in inflammation and metabolic disease. *Nat Rev Immunol* **11**, 85–97, doi: 10.1038/nri2921 (2011).
7. Lehrke, M. & Lazar, M. A. The many faces of PPAR gamma. *Cell* **123**, 993–999, doi: 10.1016/j.cell.2005.11.026 (2005).
8. Tontonoz, P., Hu, E., Graves, R. A., Budavari, A. I. & Spiegelman, B. M. Mppar-Gamma-2 - Tissue-Specific Regulator of an Adipocyte Enhancer. *Gene Dev* **8**, 1224–1234, doi: 10.1101/gad.8.10.1224 (1994).
9. Tontonoz, P. & Spiegelman, B. M. Fat and beyond: The diverse biology of PPAR gamma. *Annu Rev Biochem* **77**, 289–312, doi: 10.1146/annurev.biochem.77.061307.091829 (2008).
10. Barak, Y. *et al.* PPAR gamma is required for placental, cardiac, and adipose tissue development. *Mol Cell* **4**, 585–595, doi: 10.1016/S1097-2765(00)80209-9 (1999).

11. Hammarstedt, A., Andersson, C. X., Sopsakis, V. R. & Smith, U. The effect of PPAR gamma ligands on the adipose tissue in insulin resistance. *Prostag Leukotr Ess* **73**, 65–75, doi: 10.1016/j.plefa.2005.04.008 (2005).
12. Lehmann, J. M. *et al.* An Antidiabetic Thiazolidinedione Is a High-Affinity Ligand for Peroxisome Proliferator-Activated Receptor Gamma (Ppar-Gamma). *J Biol Chem* **270**, 12953–12956 (1995).
13. Kallen, C. B. & Lazar, M. A. Antidiabetic thiazolidinediones inhibit leptin (ob) gene expression in 3T3-L1 adipocytes. *P Natl Acad Sci USA* **93**, 5793–5796, doi: 10.1073/pnas.93.12.5793 (1996).
14. Rizos, C. V., Elisaf, M. S., Mikhailidis, D. P. & Liberopoulos, E. N. How safe is the use of thiazolidinediones in clinical practice? *Expert Opin Drug Saf* **8**, 15–32, doi: 10.1517/14740330802597821 (2009).
15. Chaggar, P. S., Shaw, S. M. & Williams, S. G. Thiazolidinediones and heart failure. *Diabetes Vasc Dis Re* **6**, 146–152, doi: 10.1177/1479164109338772 (2009).
16. Hu, E. D., Tontonoz, P. & Spiegelman, B. M. Transdifferentiation of Myoblasts by the Adipogenic Transcription Factors Ppar-Gamma and C/EBP-Alpha. *P Natl Acad Sci USA* **92**, 9856–9860, doi: 10.1073/pnas.92.21.9856 (1995).
17. Larsen, T. M., Toubro, S. & Astrup, A. PPARgamma agonists in the treatment of type II diabetes: is increased fatness commensurate with long-term efficacy? *Int J Obesity* **27**, 147–161, doi: 10.1038/sj.ijo.802223 (2003).
18. Rosen, E. D. & MacDougald, O. A. Adipocyte differentiation from the inside out. *Nat Rev Mol Cell Bio* **7**, 885–896, doi: 10.1038/nrm2066 (2006).
19. Farmer, S. R. Transcriptional control of adipocyte formation. *Cell Metab* **4**, 263–273, doi: 10.1016/j.cmet.2006.07.001 (2006).
20. Ahmadian, M. *et al.* PPAR gamma signaling and metabolism: the good, the bad and the future. *Nat Med* **19**, 557–566, doi: 10.1038/nm.3159 (2013).
21. Yu, C. *et al.* The nuclear receptor corepressors NCoR and SMRT decrease peroxisome proliferator-activated receptor gamma transcriptional activity and repress 3T3-L1 adipogenesis. *J Biol Chem* **280**, 13600–13605, doi: 10.1074/jbc.M409468200 (2005).
22. van Beekum, O., Fleskens, V. & Kalkhoven, E. Posttranslational Modifications of PPAR-gamma: Fine-tuning the Metabolic Master Regulator. *Obesity* **17**, 213–219, doi: 10.1038/oby.2008.473 (2009).
23. Anbalagan, M., Huderson, B., Murphy, L. & Rowan, B. G. Post-translational modifications of nuclear receptors and human disease. *Nucl Recept Signal* **10**, e001, doi: 10.1621/nrs.10001 (2012).
24. Hu, E. D., Kim, J. B., Sarraf, P. & Spiegelman, B. M. Inhibition of adipogenesis through MAP kinase-mediated phosphorylation of PPAR gamma. *Science* **274**, 2100–2103, doi: 10.1126/science.274.5295.2100 (1996).
25. Rangwala, S. M. *et al.* Genetic modulation of PPAR gamma phosphorylation regulates insulin sensitivity. *Dev Cell* **5**, 657–663, doi: 10.1016/S1534-5807(03)00274-0 (2003).
26. Choi, J. H. *et al.* Anti-diabetic drugs inhibit obesity-linked phosphorylation of PPAR gamma by Cdk5. *Nature* **466**, 451–U451, doi: 10.1038/nature09291 (2010).
27. Picard, F. *et al.* Sirt1 promotes fat mobilization in white adipocytes by repressing PPAR-gamma (vol 429, pg 771, 2004). *Nature* **430**, 921–921, doi: 10.1038/nature02892 (2004).
28. Yamashita, D. *et al.* The transactivating function of peroxisome proliferator-activated receptor gamma is negatively regulated by SUMO conjugation in the amino-terminal domain. *Genes Cells* **9**, 1017–1029, doi: 10.1111/j.1365-2443.2004.00786.x (2004).
29. Kim, J. H. *et al.* Suppression of PPAR gamma through MKRN1-mediated ubiquitination and degradation prevents adipocyte differentiation. *Cell Death Differ* **21**, 594–603, doi: 10.1038/cdd.2013.181 (2014).
30. Kilroy, G., Kirk-Ballard, H., Carter, L. E. & Floyd, Z. E. The Ubiquitin Ligase Siah2 Regulates PPAR gamma Activity in Adipocytes. *Endocrinology* **153**, 1206–1218, doi: 10.1210/en.2011-1725 (2012).
31. Han, L. M. *et al.* Upregulation of SIRT1 by 17 beta-estradiol depends on ubiquitin-proteasome degradation of PPAR-gamma mediated by NEDD4-1. *Protein Cell* **4**, 310–321, doi: 10.1007/s13238-013-2124-z (2013).
32. Naito, A. T. *et al.* Promotion of CHIP-Mediated p53 Degradation Protects the Heart From Ischemic Injury. *Circ Res* **106**, 1692–U1669, doi: 10.1161/Circresaha.109.214346 (2010).
33. Ahmed, S. F. *et al.* The Chaperone-assisted E3 Ligase C Terminus of Hsc70-interacting Protein (CHIP) Targets PTEN for Proteasomal Degradation. *J Biol Chem* **287**, 15996–16006, doi: 10.1074/jbc.M111.321083 (2012).
34. Petrucelli, L. *et al.* CHIP and Hsp70 regulate tau ubiquitination, degradation and aggregation. *Hum Mol Genet* **13**, 703–714, doi: 10.1093/hmg/ddh083 (2004).
35. Seo, J. *et al.* CHIP controls necroptosis through ubiquitylation- and lysosome-dependent degradation of RIPK3. *Nat Cell Biol* **18**, 291, doi: 10.1038/ncb3314 (2016).
36. Ballinger, C. A. *et al.* Identification of CHIP, a novel tetratricopeptide repeat-containing protein that interacts with heat shock proteins and negatively regulates chaperone functions. *Mol Cell Biol* **19**, 4535–4545 (1999).
37. He, B. *et al.* An androgen receptor NH2-terminal conserved motif interacts with the COOH terminus of the Hsp70-interacting protein (CHIP). *J Biol Chem* **279**, 30643–30653, doi: 10.1074/jbc.M403117200 (2004).
38. Zhang, Q. G. *et al.* C terminus of Hsc70-interacting protein (CHIP)-mediated degradation of hippocampal estrogen receptor-alpha and the critical period hypothesis of estrogen neuroprotection. *P Natl Acad Sci USA* **108**, E617–E624, doi: 10.1073/pnas.1104391108 (2011).
39. Connell, P. *et al.* The co-chaperone CHIP regulates protein triage decisions mediated by heat-shock proteins. *Nat Cell Biol* **3**, 93–96 (2001).
40. Parsons, J. L. *et al.* CHIP-mediated degradation and DNA damage-dependent stabilization regulate base excision repair proteins. *Mol Cell* **29**, 477–487, doi: 10.1016/j.molcel.2007.12.027 (2008).
41. Ferreira, J. V. *et al.* STUB1/CHIP is required for HIF1A degradation by chaperone-mediated autophagy. *Autophagy* **9**, 1349–1366, doi: 10.4161/auto.25190 (2013).
42. Paul, I., Ahmed, S. F., Bhowmik, A., Deb, S. & Ghosh, M. K. The ubiquitin ligase CHIP regulates c-Myc stability and transcriptional activity. *Oncogene* **32**, 1284–1295, doi: 10.1038/onc.2012.144 (2013).
43. Zhang, H. Q. *et al.* A Bipartite Interaction between Hsp70 and CHIP Regulates Ubiquitination of Chaperoned Client Proteins. *Structure* **23**, 472–482, doi: 10.1016/j.str.2015.01.003 (2015).
44. Kang, S. A., Cho, H. S., Yoon, J. B., Chung, I. K. & Lee, S. T. Hsp90 rescues PTK6 from proteasomal degradation in breast cancer cells. *Biochem J* **447**, 313–320, doi: 10.1042/Bj20120803 (2012).
45. Chen, F. *et al.* Opposing Actions of Heat Shock Protein 90 and 70 Regulate Nicotinamide Adenine Dinucleotide Phosphate Oxidase Stability and Reactive Oxygen Species Production. *Arterioscl Throm Vas* **32**, 2989, doi: 10.1161/Atvbaha.112.300361 (2012).
46. Nguyen, M. T., Csermely, P. & Soti, C. Hsp90 chaperones PPAR gamma and regulates differentiation and survival of 3T3-L1 adipocytes. *Cell Death Differ* **20**, 1654–1663, doi: 10.1038/cdd.2013.129 (2013).
47. Sahara, N. *et al.* In vivo evidence of CHIP up-regulation attenuating tau aggregation. *J Neurochem* **94**, 1254–1263, doi: 10.1111/j.1471-4159.2005.03272.x (2005).
48. Kilroy, G. *et al.* The ubiquitin ligase Siah2 regulates obesity-induced adipose tissue inflammation. *Obesity (Silver Spring)* **23**, 2223–2232, doi: 10.1002/oby.21220 (2015).
49. Saraf, N., Sharma, P. K., Mondal, S. C., Garg, V. K. & Singh, A. K. Role of PPARγ2 transcription factor in thiazolidinedione-induced insulin sensitization. *J Pharm Pharmacol* **64**, 161–171, doi: 10.1111/j.2042-7158.2011.01366.x (2012).
50. Soccio, R. E., Chen, E. R. & Lazar, M. A. Thiazolidinediones and the Promise of Insulin Sensitization in Type 2 Diabetes. *Cell Metab* **20**, 573–591, doi: 10.1016/j.cmet.2014.08.005 (2014).

51. Shah, P. & Mudaliar, S. Pioglitazone: side effect and safety profile. *Expert Opin Drug Saf* **9**, 347–354, doi: 10.1517/14740331003623218 (2010).
52. Nesto, R. W. *et al.* Thiazolidinedione use, fluid retention, and congestive heart failure. *Diabetes Care* **27**, 256–263, doi: 10.2337/diacare.27.1.256 (2004).
53. Wright, M. B., Bortolini, M., Tadayyon, M. & Bopst, M. Minireview: Challenges and Opportunities in Development of PPAR Agonists. *Mol Endocrinol* **28**, 1756–1768, doi: 10.1210/me.2013-1427 (2014).
54. Choi, S. S. *et al.* PPAR gamma Antagonist Gleevec Improves Insulin Sensitivity and Promotes the Browning of White Adipose Tissue. *Diabetes* **65**, 829–839, doi: 10.2337/db15-1382 (2016).
55. Abravaya, K., Myers, M. P., Murphy, S. P. & Morimoto, R. I. The Human Heat-Shock Protein Hsp70 Interacts with Hsf, the Transcription Factor That Regulates Heat-Shock Gene-Expression. *Gene Dev* **6**, 1153–1164, doi: 10.1101/gad.6.7.1153 (1992).

### Acknowledgements

This research was supported by a National Research Foundation of Korea (NRF) grant funded by the Ministry of Science, ICT, and Future Planning (NRF-2015R1A3A2066581) to J. Song, and by the National Cancer Center, Korea (NCC-1420300).

### Author Contributions

Design and conception of the study: J.-H. Kim, J.W. Song Experiments: J.-H. Kim, S. Shin, M.-S. Lee, H.-J. Han Material acquisition: J. Seo, E.-W. Lee, M. Jeong Proof reading: all authors read and approved manuscript.

### Additional Information

**Supplementary information** accompanies this paper at <http://www.nature.com/srep>

**Competing financial interests:** The authors declare no competing financial interests.

**How to cite this article:** Kim, J.-H. *et al.* C-terminus of HSC70-Interacting Protein (CHIP) Inhibits Adipocyte Differentiation via Ubiquitin- and Proteasome-Mediated Degradation of PPAR $\gamma$ . *Sci. Rep.* **7**, 40023; doi: 10.1038/srep40023 (2017).

**Publisher's note:** Springer Nature remains neutral with regard to jurisdictional claims in published maps and institutional affiliations.



This work is licensed under a Creative Commons Attribution 4.0 International License. The images or other third party material in this article are included in the article's Creative Commons license, unless indicated otherwise in the credit line; if the material is not included under the Creative Commons license, users will need to obtain permission from the license holder to reproduce the material. To view a copy of this license, visit <http://creativecommons.org/licenses/by/4.0/>

© The Author(s) 2017